Available online at www.sciencedirect.com
ScienceDirect
Journal of Nuclear Materials 367–370 (2007) 713–718
journal of nuclear materials
www.elsevier.com/locate/jnucmat

Mechanical properties of advanced SiC/SiC composites after neutron irradiation

K. Ozawa [a,*], T. Nozawa [b], Y. Katoh [b], T. Hinoki [c], A. Kohyama [c]

[a] Graduate School of Energy Science, Kyoto University, Gokasho, Uji, Kyoto 611-0011, Japan
[b] Materials Science and Technology Division, Oak Ridge National Laboratory, P.O. Box 2008, Oak Ridge, TN 37831-6138, USA
[c] Institute of Advanced Energy, Kyoto University, Gokasho, Uji, Kyoto 611-0011, Japan

Abstract

The effect of neutron irradiation on tensile properties in advanced 2D-SiC/SiC composites was evaluated. The composites used were composed of a SiC matrix obtained by the forced-flow chemical vapor infiltration (FCVI) process and either Tyranno™-SA Grade-3 or Hi-Nicalon™ Type-S fibers with single-layered PyC coating as the interphase. Neutron irradiation fluence and temperature were 3.1×10^{25} n/m^2 ($E > 0.1$ MeV) and 1.2×10^{26} n/m^2 at 740–750 °C. Tensile properties were evaluated by cyclic tensile test, and hysteresis loop analysis was applied in order to evaluate interfacial properties. Both composites exhibited excellent irradiation resistance in ultimate and proportional limit tensile stresses. From the hysteresis loop analysis, the level of interfacial sliding stress decreased significantly after irradiation to 1.5×10^{26} n/m^2 at 750 °C.

1. Introduction

Silicon carbide (SiC) continuous fiber-reinforced SiC matrix composites (SiC/SiC composites) are attractive structural materials for fusion reactors and advanced fission reactors because of their superior mechanical properties and good irradiation resistance at high temperatures [1]. The mechanical properties of SiC/SiC composites after irradiation is determined by the properties of their constituents, especially the fiber/matrix (F/M) interphase in case of composites with high modulus matrix. In earlier studies, SiC/SiC composites reinforced with nano-crystalline and non-stoichiometric SiC fibers have shown interfacial debonding due primarily to fiber contraction, which caused severe degradation in flexural strength [2–5]. In recent studies, however, advanced SiC/SiC composites appeared to retain ultimate flexural strength due to improved irradiation stability of the high crystallinity and near-stoichiometric SiC fibers [5,6].

For composites with highly irradiation-resistant matrices and fibers, irradiation effects on F/M interfacial properties has become one of the most important issues to be investigated. However, it is difficult to use the simple flexural testing to develop an understanding of irradiation effects on interfacial properties, because it is hard to analyze the data due to mixed failure modes. Simple failure modes, such as are obtained in tensile tests enable the

* Corresponding author. Tel.: +81 774 38 3466; fax: +81 774 38 3467.
E-mail address: kazumi@iae.kyoto-u.ac.jp (K. Ozawa).

0022-3115/$ - see front matter © 2007 Elsevier B.V. All rights reserved.
doi:10.1016/j.jnucmat.2007.03.033

fracture behavior of SiC/SiC composites after irradiation to be understood more precisely. Recent studies have employed tests yielding simple failure modes to evaluate interfacial properties [7–9].

The main purpose of this work is to identify neutron irradiation effects on tensile and interfacial properties of advanced SiC/SiC composites reinforced with two commercially available, high crystallinity, near-stoichiometric SiC fibers. For this purpose, tensile properties were evaluated in an unloading/reloading cyclic tensile test and the hysteresis loop analysis method was applied to predict interfacial properties.

2. Experimental procedure

The composites used in this study were produced thorough a forced-flow thermal gradient chemical vapor infiltration (FCVI) process developed at Oak Ridge National Laboratory. Either Tyranno™-SA 3rd grade (hereafter TySA) or Hi-Nicalon™ Type-S (hereafter HNLS) fibers were used as reinforcements. These were stacked in a [0°/90°] orientation and held tightly in a graphite fixture for interphase deposition and subsequent matrix dentification. The F/M interphase was singly-layered pyrolytic carbon (PyC) and the thickness was 20–60 nm. The density of the composites was 2.3–2.7 g/cm^3, and the fiber volume fraction and porosity were ~38% and 17–25%, respectively. More detailed information about the materials fabrication is given elsewhere [10,11].

Neutron irradiation was performed in JOYO fast spectrum reactor at Oarai, Japan, in JNC-54 and -61 capsules as part of the CMIR-6 irradiation campaign. Neutron fluence and irradiation temperature were 3.1×10^{25} n/m^2 ($E>0.1$ MeV) at 740 °C and 1.2×10^{26} n/m^2 at 750 °C. An equivalence of one displacement per atom (dpa) $=1\times10^{25}$ n/m^2 ($E>0.1$ MeV) is assumed in the following sections. The irradiation temperature was passively controlled by a fixed composition gas gap technique.

Tensile tests were conducted in accordance with ASTM C1275 at room temperature under crosshead displacement control at 0.5 mm/min by using a face-loaded miniature specimen developed previously [12,13]. The gauge dimensions were $3\times1.5\times15$ mm and the specimen machining involved surface grinding into fabric layers [10]. A 1.0 mm-thick aluminum tab was attached to each end of the rectangular specimens, and a pair of 6.0 mm-length strain gauges were adhered in the center of gauge sections on both sides. Specimens were mounted in the test frame by connection of a wedge-type gripping system that was kept in the plastic bags during the test. Successful tests typically retained intact tab adhesion to the samples. In order to avoid fractional bending during the tests, both sides of the wedge fixture were fixed at 60 kN m equally using a torque driver. The detailed tensile setup is given elsewhere [7].

After the tensile tests, the fractured surfaces of the specimens were observed using an optical microscope and scanning electron microscope (SEM).

3. Results

Fig. 1 exhibits typical tensile stress–strain curves of TySA and HNLS composites after neutron irradiation. The composites in all conditions exhibited quasi-ductile behaviors. There was an initial steeper linear region in the stress–strain curve, with a second, nearly linear region at higher strains during tensile loading with multiple unloading/reloading sequences. The initial linear portion corresponds to the linear elastic deformation of the composite,

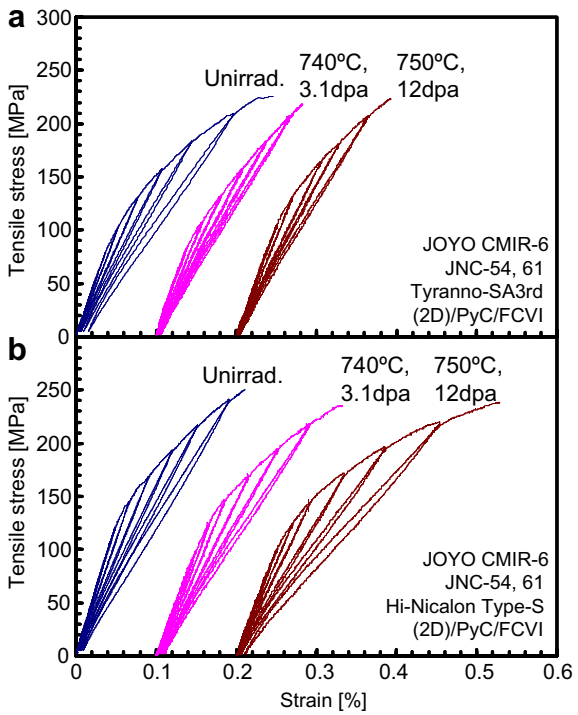

Fig. 1. Representative tensile stress–strain curves and hysteresis loops for (a) TySA (2D)/PyC/FCVI, (b) HNLS (2D)/PyC/FCVI composites after neutron irradiation.

whereas the second linear portion corresponds to a process of progressive development and opening of the multiple matrix micro-cracks.

Table 1 lists a summary of unirradiated and irradiated tensile properties: proportional limit stress (PLS), ultimate tensile stress (UTS) and elastic modulus (E) obtained from the tensile tests, and Fig. 2 shows the tensile properties after neutron irradiation. Both composites exhibited excellent irradiation resistance. Almost no degradation in PLS and UTS

Table 1
Summary of unirradiated and irradiated tensile properties

ID	Irradiation condition	E (GPa)	PLS (MPa)	UTS (MPa)	Number of test
#1266	Unirrad.	257 (32)	76 (31)	218 (18)	6
	740 °C, 3.1 dpa	216 (11)	80 (9)	241 (30)	3
	750 °C, 12 dpa	198 (19)	112 (12)	209 (11)	3
#1272	Unirrad.	253 (25)	98 (17)	227 (27)	10
	740 °C, 3.1 dpa	222 (33)	107 (9)	210 (18)	3
	750 °C, 12 dpa	200 (5)	100 (18)	220 (16)	4

Numbers in parenthesis show standard deviations. #1266, TySA (2D)/PyC/FCVI; #1272, HNLS (2D)/PyC/FCVI; E, tensile elastic modulus; PLS, proportional limit stress; UTS, ultimate tensile strength.

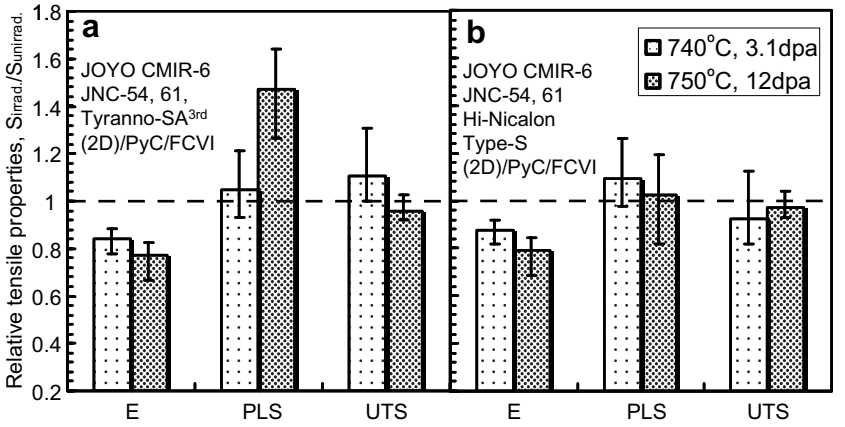

Fig. 2. Ratio of irradiated to unirradiated tensile properties of (a) TySA (2D)/PyC/FCVI, (b) HNLS (2D)/PyC/FCVI composites after neutron irradiation. Error bars show maximum and minimum.

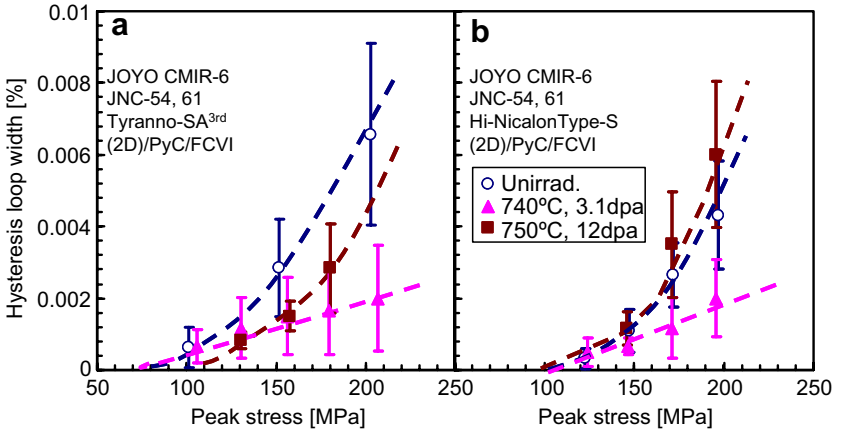

Fig. 3. Hysteresis loop width plotted against peak stress; (a) TySA (2D)/PyC/FCVI, (b) HNLS (2D)/PyC/FCVI composites. Error bars show standard deviation.

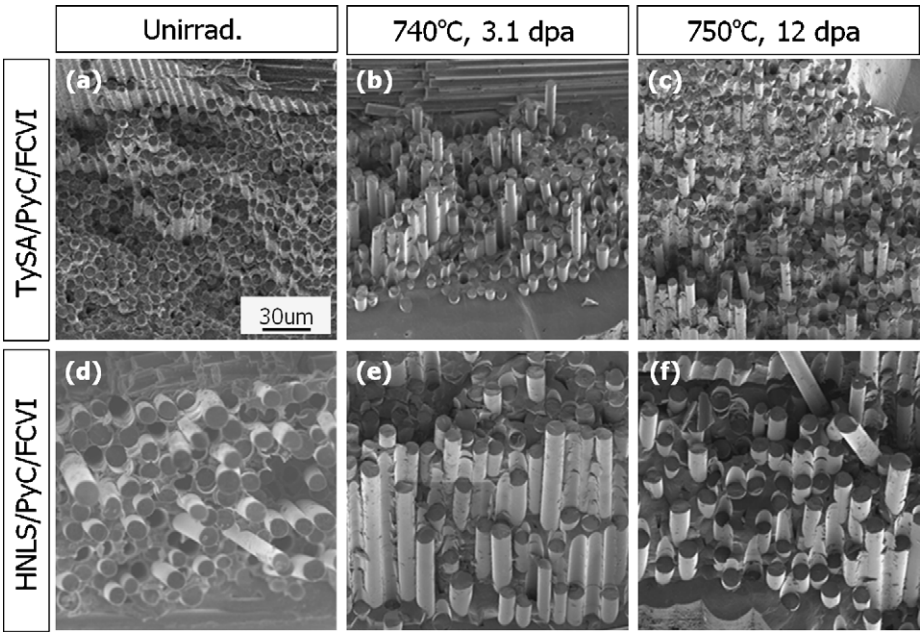

Fig. 4. Typical fracture surfaces of unirradiated and neutron-irradiated tensile specimens; (a) unirradiated, (b) 740 °C, 3.1 dpa and (c) 750 °C, 12 dpa for TySA (2D)/PyC/FCVI, and (d) unirradiated, (e) 740 °C, 3.1 dpa and (f) 750 °C, 12 dpa for HNLS (2D)/PyC/FCVI.

occurred under both irradiation conditions, and an increase of about 50% was measured in PLS of TySA composites irradiated to 12 dpa at 750 °C. In elastic modulus, a 15–20% decrease was obtained for both composites.

Fig. 3 exhibits the maximum hysteresis loop width at each peak stress where σ_p is the transition stress from reloading to unloading. For both composites, the hysteresis loop width after irradiation up to 3.1 dpa became narrower than that of the unirradiated one. After neutron irradiation to 12 dpa, the hysteresis loop width of TySA composites remained narrower, while that of HNLS exhibited almost the same behavior as the unirradiated material.

Fig. 4 exhibits typical fracture surfaces of composites observed by SEM. No significant change of fiber pull-out was observed for both composites after irradiation. Fiber pull-out in TySA composites were shorter than that in HNLS composites under all conditions.

4. Discussion

Both composites irradiated to 3.1 dpa at 740 °C exhibited narrower hysteresis loop widths, a slightly steeper slope in the second linear portion of the curve and nearly unchanged fiber pull-out length, all of which imply retaining or increasing of interfacial sliding stress.

For further investigation of interfacial properties, the method of unloading/reloading hysteresis loop analysis methodology proposed by Vagaggini, Domergue and Evance was applied [14–17]. In this analysis, the inelastic strain index, which is the most important parameter for estimating interfacial properties, and Young's modulus of the material with matrix cracks were obtained from values of the inverse tangent moduli of reloading tensile stress–strain curves at different peak stress. A detailed description of this analysis method for 2D composites is found elsewhere [17].

The maximum hysteresis loop width ($\delta_{\max}$) before and after irradiation is dependent on both interfacial sliding stress (τ) and mean matrix crack spacing ($\bar{d}$). The composites in all conditions met the large debond energy condition. For this condition, the maximum hysteresis loop width ($\delta_{\max}$) is given by [14,17],

$$\delta_{\max} = 4\lambda\sigma_p^2\left(1-\frac{\sigma_i}{\sigma_p}\right)^2 = \frac{b_2(1-a_1 f)^2}{f^2\tau E_m}\frac{R}{\bar{d}}\sigma_p^2\left(1-\frac{\sigma_i}{\sigma_p}\right)^2, \quad \text{for } \sigma_i/\sigma_p \cong 0.85, \tag{1}$$

where λ is inelastic strain index, σ_i is 'debond' stress [14], E_m is Young's modulus of matrix, R is fiber radius, f is fiber volume fraction, and a_1 and b_1 are the Hutchinson–Jensen parameters [18]. All the parameters except interfacial sliding stress and mean matrix crack spacing remain almost unchanged during irradiation.

Unfortunately, the mean matrix crack spacing was not measured, so the interfacial sliding stress parameter $\tau' = \tau \cdot \bar{d}/R$ obtained from the inelastic strain index was used for this analysis. Thus, the evaluation of interfacial sliding stress parameter at the same matrix crack spacing (i.e. same matrix damage level) is required. The matrix damage parameter (D) is defined as [14],

$$D \equiv \frac{E - E^*}{E^*} = B\frac{R}{\bar{d}}, \tag{2}$$

where E is the elastic modulus of the composite, E^* is Young's modulus of the composite with matrix cracks obtained from the reloading stress–strain curve, and B is a constant for particular composite. As shown in Eq. (2), the matrix damage parameter is inversely proportional to matrix crack spacing. Therefore, the interfacial sliding stress can be predicted using the interfacial sliding stress parameter obtained for the same matrix damage parameter.

Fig. 5 exhibits the interfacial sliding stress parameter at approximately the same matrix damage parameter ($D \cong 0.2$). For both composites, the interfacial sliding stress parameter remained nearly constant after irradiation up to 3.1 dpa at 740 °C, while the parameter decreased after irradiation up to 12 dpa at 750 °C.

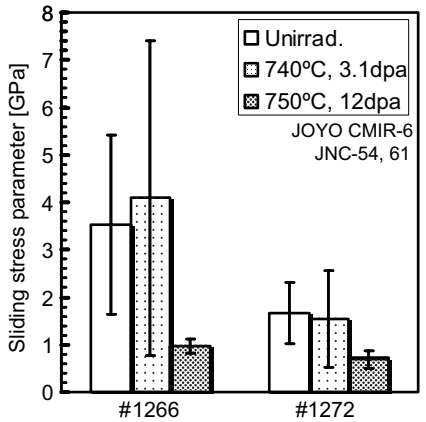

Fig. 5. Interfacial sliding stress parameters compared at similar matrix damage parameters for composite samples before and after neutron irradiation. #1266; TySA (2D)/PyC/FCVI, #1272; HNLS (2D)/PyC/FCVI. Error bars show standard deviation.

According to the work by Bokros et al. [19,20], the interfacial PyC is expected to shrink in both the a and c axis directions after neutron irradiation up to $2–3 \times 10^{25}$ n/m^2 in the range of 520–690 °C. However, it began to swell significantly in the c axis direction over $\sim 10 \times 10^{25}$ n/m^2 irradiation. This result might be correlated with the analysis of data in this study, but the details are unclear. Therefore, further research and SEM observations of crack propagation and TEM observation of the PyC interphase itself are required in order to understand the behavior of the interphase after neutron irradiation.

Residual stress between the fiber and matrix may affect the tensile behavior of SiC/SiC composites, so the misfit stress σ^T was also estimated by hysteresis loop analysis. The conversion of misfit stress to residual stress components was carried out by the method discussed elsewhere [14]. At high peak stresses, the misfit stress was influenced by fiber roughness due to the damage of the PyC interphase during the test. Therefore, the misfit stress at a peak stress of 125–175 MPa was used for this evaluation. The result is: $\sigma^T = +9 \pm 6$ MPa (unirradiated), $+3 \pm 3$ MPa (3.1 dpa at 740 °C), $+6 \pm 2$ MPa (12 dpa at 750 °C) for TySA composites, and $+9 \pm 5$ MPa, $+6 \pm 5$ MPa, $+5 \pm 3$ MPa for HNLS composites. From these results, it appears that the misfit stress may not affect the tensile behavior of either composites under these irradiation conditions.

5. Summary

In order to identify the effects of neutron irradiation on tensile properties of advanced SiC/SiC composites (Tyranno-SA3rd (2D)/PyC/FCVI and Hi-Nicalon Type-S (2D)/PyC/FCVI), unloading/reloading cyclic tensile tests were conducted and hysteresis loop analysis was applied. Neutron fluence and irradiation temperature were 3.1×10^{25} n/m^2 ($E > 0.1$ MeV) and 1.2×10^{26} n/m^2 at 740–750 °C. The following results were obtained:

1. Both composites exhibited excellent irradiation resistance to changes in ultimate tensile strength and proportional limit stress. A slight reduction of elastic modulus was observed after irradiation.

2. Hysteresis loop analysis indicated that the sliding stress at fiber/matrix interfaces remained almost unchanged after irradiation to 3.1×10^{25} n/m^2 at 740 °C, whereas it was significantly reduced by 12×10^{25} n/m^2 at 750 °C for both composites.

Acknowledgements

This work was performed as a part of a corroboration at the Irradiation Experimental Facility, Institute for Materials Research, Tohoku University, Japan. Materials were supplied as part of the DOE/MEXT JUPITER-II Collaboration for Development of Advanced Blanket Performance under Irradiation and System Integration.

References

[1] Y. Katoh, L.L. Snead, C.H. Henager Jr., A. Hasegawa, A. Kohyama, B. Riccardi, H. Hegeman, J. Nucl. Mater., in press, doi:10.1016/j.jnucmat.2007.03.032.
[2] L.L. Snead, M.C. Osborne, R.A. Lowden, J. Strizak, R.J. Shinavski, K.L. More, W.S. Eatherly, J. Bailey, A.M. Williams, J. Nucl. Mater. 253 (1998) 20.
[3] G.W. Hollenberg, C.H. Henager Jr., G.E. Youngblood, D.J. Trimble, S.A. Simonson, G.A. Newsome, E. Lewis, J. Nucl. Mater. 219 (1995) 70.
[4] A.J. Frias Rebelo, H.W. Scholz, H. Kolbe, G.P. Tartagalia, P. Fenici, J. Nucl. Mater. 258–263 (1998) 1582.
[5] L.L. Snead, Y. Katoh, A. Kohyama, J.L. Bailey, N.L. Vaughn, R.A. Lowden, J. Nucl. Mater. 283–287 (2000) 551.
[6] T. Hinoki, L.L. Snead, Y. Katoh, A. Hasegawa, T. Nozawa, A. Kohyama, J. Nucl. Mater. 283–287 (2002) 1157.
[7] T. Nozawa, K. Ozawa, S. Kondo, T. Hinoki, L.L. Snead, A. Kohyama, J. ASTM Int. 2 (2005) 12884-1.
[8] K. Ozawa, T. Hinoki, T. Nozawa, Y. Katoh, Y. Maki, S. Kondo, S. Ikeda, A. Kohyama, Mater. Trans. 47 (2006) 207.
[9] Y. Katoh, T. Nozawa, L.L. Snead, T. Hinoki, J. Nucl. Mater., in press, doi:10.1016/j.jnucmat.2007.03.083.
[10] Y. Katoh, T. Nozawa, L.L. Snead, J. Am. Ceram. Soc. 88 (2005) 3088.
[11] Y. Katoh, L.L. Snead, T. Hinoki, A. Kohyama, N. Igawa, T. Taguchi, Mater. Trans. 46 (2005) 527.
[12] T. Nozawa, Y. Katoh, A. Kohyama, E. Lara-Curzio, Ceram. Eng. Sci. Proc. 24 (2003) 415.
[13] T. Nozawa, E. Lara-Curzio, Y. Katoh, A. Kohyama, Ceram. Trans. 144 (2002) 245.
[14] E. Vagaggini, J.-M. Domergue, A.G. Evans, J. Am. Ceram. Soc. 78 (1995) 2709.
[15] A.G. Evans, J.-M. Domergue, E. Vagaggini, J. Am. Ceram. Soc. 77 (1994) 1425.
[16] J.-M. Domergue, E. Vagaggini, A.G. Evans, J. Am. Ceram. Soc. 78 (1995) 2721.
[17] J.-M. Domergue, F.E. Heredia, A.G. Evans, J. Am. Ceram. Soc. 79 (1996) 161.
[18] J.W. Hutchinson, H. Jensen, Mech. Mater. 9 (1990) 139.
[19] J.C. Bokros, G.L. Gthrie, R.W. Dunlap, A.S. Schwartz, J. Nucl. Mater. 31 (1969) 25.
[20] CEGA, Report CEGA-002820, Rev 1, July 1993.